

## ${}^7\text{Be}(p,\gamma){}^8\text{B}$ S-factor from *ab initio* wave functions

P. Navrátil<sup>a</sup>\*, C. A. Bertulani<sup>b†</sup>, E. Caurier<sup>c</sup>

<sup>a</sup>Lawrence Livermore National Laboratory, P.O. Box 808, L-414, Livermore, CA 94551, USA

<sup>b</sup>Department of Physics, University of Arizona, Tucson, AZ 85721, USA

<sup>c</sup>Institut de Recherches Subatomiques (IN2P3-CNRS-Université Louis Pasteur) Batiment 27/1,67037 Strasbourg Cedex 2, France

There has been a significant progress in *ab initio* approaches to the structure of light nuclei. Starting from realistic two- and three-nucleon interactions the *ab initio* no-core shell model (NCSM) predicts low-lying levels in *p*-shell nuclei. It is a challenging task to extend *ab initio* methods to describe nuclear reactions. We present here a brief overview of the the first steps taken toward nuclear reaction applications. In particular, we discuss our calculation of the  ${}^7\text{Be}(p,\gamma){}^8\text{B}$  S-factor. We also present our first results of the  ${}^3\text{He}(\alpha,\gamma){}^7\text{Be}$  S-factor and of the S-factor of the mirror reaction  ${}^3\text{H}(\alpha,\gamma){}^7\text{Li}$ . The  ${}^7\text{Be}(p,\gamma){}^8\text{B}$  and  ${}^3\text{He}(\alpha,\gamma){}^7\text{Be}$  reactions correspond to the most important uncertainties in solar model predictions of neutrino fluxes.

### 1. INTRODUCTION

The  ${}^7\text{Be}(p,\gamma){}^8\text{B}$  capture reaction serves as an important input for understanding the solar neutrino flux [1]. Recent experiments have determined the neutrino flux emitted from  ${}^8\text{B}$  with a precision of 9% [2]. On the other hand, theoretical predictions have uncertainties of the order of 20% [3,4]. The theoretical neutrino flux depends on the  ${}^7\text{Be}(p,\gamma){}^8\text{B}$  S-factor. Many experimental and theoretical investigations studied this reaction. Experiments were performed using direct techniques with proton beams and  ${}^7\text{Be}$  targets [5–7] as well as by indirect methods when a  ${}^8\text{B}$  beam breaks up into  ${}^7\text{Be}$  and proton [8]. Theoretical calculations needed to extrapolate the measured S-factor to the astrophysically relevant Gamow energy were performed with several methods: the R-matrix parametrization [9], the potential model [10–12], and the microscopic cluster models [13–15].

In this work, we discuss the first calculation of the  ${}^7\text{Be}(p,\gamma){}^8\text{B}$  S-factor starting from *ab initio* wave functions of  ${}^8\text{B}$  and  ${}^7\text{Be}$ . It should be noted that the aim of *ab initio* approaches is to predict correctly absolute cross sections (S-factors), not only relative cross sections.

\*This work was partly performed under the auspices of the U. S. Department of Energy by the University of California, Lawrence Livermore National Laboratory under contract No. W-7405-Eng-48. Support from the LDRD contract No. 04-ERD-058, and from U.S. Department of Energy, Office of Science, (Work Proposal Number SCW0498), is acknowledged.

†Support from the grant No. DE-FG02-04ER41338 is acknowledged.

We apply the *ab initio* no-core shell model (NCSM) [16]. In this method, one considers nucleons interacting by high-precision nucleon-nucleon (NN) potentials. There are no adjustable or fitted parameters. We note that full details of our  ${}^7\text{Be}(p,\gamma){}^8\text{B}$  investigation were published in Refs. [17,18].

Another capture reaction important for our understanding of the solar model and its predictions of the neutrino fluxes is the  ${}^3\text{He}(\alpha,\gamma){}^7\text{Be}$  reaction. In this contribution we present our first results of the S-factor calculation of this reaction and of its mirror reaction  ${}^3\text{H}(\alpha,\gamma){}^7\text{Li}$  using the *ab initio* NCSM wave functions of the  ${}^7\text{Be}$ ,  ${}^7\text{Li}$ ,  ${}^3\text{He}$ ,  ${}^3\text{H}$  and  ${}^4\text{He}$  bound states.

## 2. BOUND-STATE WAVE FUNCTION AND OVERLAP FUNCTION CALCULATION

We studied the binding energies and other nuclear structure properties of  ${}^7\text{Be}$ ,  ${}^8\text{B}$  as well as  ${}^7,{}^8\text{Li}$ , and calculated overlap integrals for the  ${}^8\text{B}$  and  ${}^7\text{Be}$  bound states. Our calculations for both  $A = 7$  and  $A = 8$  nuclei were performed using the high-precision CD-Bonn 2000 NN potential [19] in model spaces up to  $10\hbar\Omega$  ( $N_{\text{max}} = 10$ ) for a wide range of HO frequencies. We then selected the optimal HO frequency corresponding to the ground-state (g.s.) energy minimum in the  $10\hbar\Omega$  space, here  $\hbar\Omega = 12$  MeV, and performed a  $12\hbar\Omega$  calculation to obtain the g.s. energy and the point-nucleon radii. The overlap integrals as well as other observables were, however, calculated only using wave functions from up to  $10\hbar\Omega$  spaces. The g.s. energies, radii and electromagnetic observables are summarized in Table 1 of Ref. [17]. Note that the CD-Bonn 2000 underbinds  ${}^7\text{Be}$ ,  ${}^8\text{B}$  and  ${}^7,{}^8\text{Li}$  by about 3–5 MeV and predicts  ${}^8\text{B}$  unbound, contrary to experiment. This suggests that the three-nucleon interaction is essential to accurately reproduce the experimental threshold. However, since the HO basis has the incorrect asymptotic behavior in the first place, we make use of only the interior part of our *ab initio* wave functions, which are likely unaffected by mild variations in the threshold value.

Concerning the excitation energies, we obtained the same level ordering for  ${}^7\text{Be}$  and  ${}^7\text{Li}$ . Our CD-Bonn 2000 ordering is in agreement with experiment for the 9 lowest levels in  ${}^7\text{Li}$ . In  ${}^7\text{Be}$ , the experimental  $7/2_2^-$  and  $3/2_2^-$  levels are reversed compared to our results and to the situation in  ${}^7\text{Li}$ . While for the magnetic moments and M1 transitions we obtained a very small dependence of the calculated values on the HO frequency or the basis size, the radii and quadrupole moments in general increase with increasing basis size and decreasing frequency. The fastest convergence for the radii and quadrupole moment occurs at a smaller HO frequency. In our calculations with  $\hbar\Omega = 11$  and 12 MeV, the radii are close to experimental values.

From the obtained  ${}^8\text{B}$  and  ${}^7\text{Be}$  wave functions, we calculate the channel cluster form factors (overlap functions, overlap integrals)  $g_{(l\frac{1}{2})j;A-1\alpha I_1}^{A\lambda J}(r)$  following Ref. [20]. Here,  $A = 8$ ,  $l$  is the channel relative orbital angular momentum and  $\vec{r} = \left[ \frac{1}{A-1}(\vec{r}_1 + \vec{r}_2 + \dots + \vec{r}_{A-1}) - \vec{r}_A \right]$  describes the relative distance between the proton and the center of mass of  ${}^7\text{Be}$ . A conventional spectroscopic factor is obtained as  $S_{(l\frac{1}{2})j;A-1\alpha I_1}^{A\lambda J} = \int dr r^2 |g_{(l\frac{1}{2})j;A-1\alpha I_1}^{A\lambda J}(r)|^2$ . Our selected spectroscopic factors are summarized in Table 2 of Ref. [17]. We found a very weak dependence of the spectroscopic factors on the basis size and the HO frequency.

The two most important channels are the  $p$ -waves,  $l = 1$ , with the proton in the  $j = 3/2$  and  $j = 1/2$  states,  $\vec{j} = \vec{l} + \vec{s}$ ,  $s = 1/2$ . In these channels, we obtain the spectroscopic factors of 0.96 and 0.10, respectively. The dominant  $j = 3/2$  (the less important  $j = 1/2$ ) overlap integral is presented in the left (right) panel of Fig. 1 by the full line. The CD-Bonn 2000 NN potential, the  $10\hbar\Omega$  model space and the HO frequency of  $\hbar\Omega = 12$  MeV were used. Despite the fact, that a very large basis was employed in the present calculation, it is apparent that the overlap function is nearly zero at about 10 fm. This is a consequence of the HO basis asymptotics. The proton capture on  ${}^7\text{Be}$  to the weakly bound ground state of  ${}^8\text{B}$  associated dominantly by the  $E1$  radiation is a peripheral process. Consequently, the overlap integral with an incorrect asymptotic behavior cannot be used to calculate the S-factor.

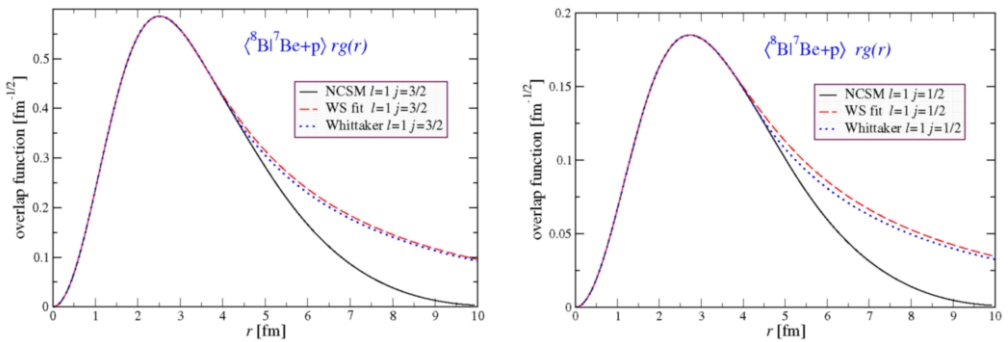


Figure 1. Overlap function,  $rg(r)$ , for the ground state of  ${}^8\text{B}$  with the ground state of  ${}^7\text{Be}$  plus proton as a dependence on separation between the  ${}^7\text{Be}$  and the proton. Left (right), the  $p$ -wave channel with  $j = 3/2$  ( $j = 1/2$ ) is shown. The full line represents the NCSM result obtained using the CD-Bonn 2000 NN potential, the  $10\hbar\Omega$  model space and the HO frequency of  $\hbar\Omega = 12$  MeV. The dashed lines represent corrected overlaps obtained from a Woods-Saxon potential whose parameters were fit to the NCSM overlaps up to 4.0 fm under the constraint to reproduce the experimental separation energy. The dotted lines represent overlap corrections by the direct Whittaker function matching.

We expect, however, that the interior part of the overlap function is realistic. It is then straightforward to correct its asymptotics. One possibility we explored utilizes solutions of a Woods-Saxon (WS) potential. In particular, we performed a least-square fit of a WS potential solution to the interior of the NCSM overlap in the range of 0 – 4 fm. The WS potential parameters were varied in the fit under the constraint that the experimental separation energy of  ${}^7\text{Be}+p$ ,  $E_0 = 0.137$  MeV, was reproduced. In this way we obtain a perfect fit to the interior of the overlap integral and a correct asymptotic behavior at the same time. The result is shown in Fig. 1 by the dashed line.

Another possibility is a direct matching of logarithmic derivatives of the NCSM overlap integral and the Whittaker function:  $\frac{d}{dr} \ln(rg_{ij}(r)) = \frac{d}{dr} \ln(C_{ij}W_{-\eta, l+1/2}(2k_0r))$ , where  $\eta$  is

the Sommerfeld parameter,  $k_0 = \sqrt{2\mu E_0}/\hbar$  with  $\mu$  the reduced mass and  $E_0$  the separation energy. Since asymptotic normalization constant (ANC)  $C_{lj}$  cancels out, there is a unique solution at  $r = R_m$ . For the discussed overlap presented, e.g. in the left panel of Fig. 1, we found  $R_m = 4.05$  fm. The corrected overlap using the Whittaker function matching is shown in Fig. 1 by a dotted line. In general, we observe that the approach using the WS fit leads to deviations from the original NCSM overlap starting at a smaller radius. In addition, the WS solution fit introduces an intermediate range from about 4 fm to about 6 fm, where the corrected overlap deviates from both the original NCSM overlap and the Whittaker function. Perhaps, this is a more realistic approach compared to the direct Whittaker function matching. In any case, by considering the two alternative procedures we are in a better position to estimate uncertainties in our S-factor results.

In the end, we re-scale the corrected overlap functions to preserve the original NCSM spectroscopic factors (Table 2 of Ref. [17]). In general, we observe a faster convergence of the spectroscopic factors than that of the overlap functions. The corrected overlap function should represent the infinite space result. By re-scaling a corrected overlap function obtained at a finite  $N_{\max}$ , we approach faster the infinite space result. At the same time, by re-scaling we preserve the spectroscopic factor sum rules.

The range used in the least-square fit is not arbitrary but varies from channel to channel. The aim is to use as large range as possible, while at the same time preserve the NCSM overlap integral as accurately as possible in that range. Concerning the discussed example (dashed lines in Fig. 1), we note that extending the range beyond 4 fm leads to a worse fit. Finally, we note that the alternative procedure of the direct Whittaker function matching is completely unique.

### 3. ${}^7\text{Be}(p,\gamma){}^8\text{B}$ S-FACTOR

The S-factor for the reaction  ${}^7\text{Be}(p,\gamma){}^8\text{B}$  also depends on the continuum wave function,  $R_{lj}^{(c)}$ . As we have not yet developed an extension of the NCSM to describe continuum wave functions, we obtain  $R_{lj}^{(c)}$  for  $s$  and  $d$  waves from a WS potential model. Since the largest part of the integrand stays outside the nuclear interior, one expects that the continuum wave functions are well described in this way. In order to have the same scattering wave function in all the calculations, we chose a WS potential from Ref. [21] that was fitted to reproduce the  $p$ -wave  $1^+$  resonance in  ${}^8\text{B}$ . It was argued [10] that such a potential is also suitable for the description of  $s$ - and  $d$ -waves. We note that the S-factor is very weakly dependent on the choice of the scattering-state potential (using our fitted potential for the scattering state instead changes the S-factor by less than 1.5 eV b at 1.6 MeV with no change at 0 MeV).

Our obtained S-factor is presented in Figs. 2 where contribution from the two partial waves are shown together with the total result (left figure). It is interesting to note a good agreement of our calculated S-factor with the recent Seattle direct measurement [7]. The sensitivity of the S-factor to the size of the NCSM basis is also presented in Figs. 2 (right figure). The overlap integrals were obtained in 6, 8 and  $10\hbar\Omega$  calculations and independently corrected to insure the proper asymptotic behavior. The same scattering states were used in all three cases. It is apparent that the sensitivity to the basis change is rather moderate. We observe a small oscillation at this frequency ( $\hbar\Omega = 12$  MeV).

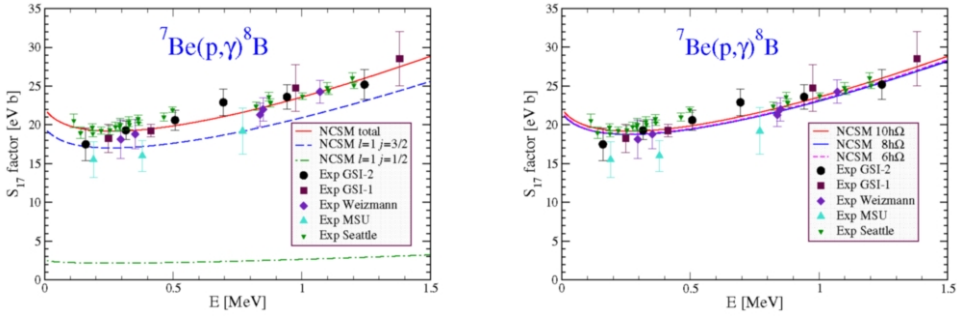


Figure 2. The  ${}^7\text{Be}(p,\gamma){}^8\text{B}$  S-factor obtained using the NCSM overlap functions with corrected asymptotics as described in the text. Left, the dashed and dashed-dotted lines show the contribution due to the  $l = 1$ ,  $j = 3/2$  and  $j = 1/2$  partial waves, respectively. Right, the dependence on the size of the basis form  $6\hbar\Omega$  to  $10\hbar\Omega$  is shown. Experimental values are from Refs. [7,8].

In order to judge the convergence of our S-factor calculation, we performed a detailed investigation of the model-space-size and the HO frequency dependencies. We used the HO frequencies in the range from  $\hbar\Omega = 11$  MeV to  $\hbar\Omega = 15$  MeV and the model spaces from  $6\hbar\Omega$  to  $10\hbar\Omega$ . Using the WS solution fit procedure to correct the asymptotics of the NCSM overlap functions, we obtain basically identical energy dependence in all cases. The absolute values of the S-factor increase with decreasing frequency. To determine the optimal frequency and interpolate the converged S-factor result, we examined the basis size dependence for different HO frequencies. In the case of the  $\hbar\Omega = 15$  MeV frequency, we observe a steady increase of the S-factor with model space size enlargement from  $6\hbar\Omega$  to  $10\hbar\Omega$ . Contrary to this situation, the calculation using the HO frequency of  $\hbar\Omega = 11$  MeV shows that the S-factor does not increase any more with increasing  $N_{\text{max}}$ . Actually, there is a small decrease when going from the  $8\hbar\Omega$  to the  $10\hbar\Omega$ . In addition to the results obtained using the WS solution fit procedure, we also investigated the  $S_{17}$  using the alternative direct Whittaker matching procedure. In general, both procedures lead to basically identical energy dependence with a difference of about 1 to 2 eV b in the S-factor with the smaller values from the direct Whittaker function matching procedure. Taking into account that in the case of the direct Whittaker function matching the  $S_{17}$  increases with  $N_{\text{max}}$  even at the HO frequency of  $\hbar\Omega = 11$  MeV, unlike in the case of the WS solution fit procedure, results of the two approaches do not contradict each other. Combining all these results, we determine that the optimal frequency is between  $\hbar\Omega = 11$  and 12 MeV. Results in this frequency region show very weak dependence on  $N_{\text{max}}$ , with relative difference between the two methods always in the range of 5 to 8%. The full range of results is covered by  $S_{17}(10 \text{ keV}) = 22.1 \pm 1.0$  eV b.

#### 4. ${}^3\text{He}(\alpha,\gamma){}^7\text{Be}$ S-FACTOR

The  ${}^3\text{He}(\alpha,\gamma){}^7\text{Be}$  capture reaction cross section was identified the most important uncertainty in the solar model predictions of the neutrino fluxes in the p-p chain [4]. We investigated the bound states of  ${}^7\text{Be}$ ,  ${}^3\text{He}$  and  ${}^4\text{He}$  within the *ab initio* NCSM and calculated the overlap functions of  ${}^7\text{Be}$  bound states with the ground states of  ${}^3\text{He}$  plus  ${}^4\text{He}$  as a function of separation between the  ${}^3\text{He}$  and the  $\alpha$  particle. The obtained  $p$ -wave overlap functions of the  ${}^7\text{Be}$   $3/2^-$  ground state and the  ${}^7\text{Be}$   $1/2^-$  excited state are presented in the left and right panel, respectively, of Fig. 3 by the full lines. The dashed lines show the corrected overlap functions obtained by the least-square fits of the WS parameters done in the same way as in the  ${}^8\text{B}\leftrightarrow{}^7\text{Be}+p$  case. The corresponding NCSM spectroscopic factors obtained using the CD-Bonn 2000 in the  $10\hbar\Omega$  model space for  ${}^7\text{Be}$  ( $12\hbar\Omega$  for  ${}^3,{}^4\text{He}$ ) and HO frequency of  $\hbar\Omega = 13$  MeV are 0.93 and 0.91 for the ground state and the first excited state of  ${}^7\text{Be}$ , respectively. We note that contrary to the  ${}^8\text{B}\leftrightarrow{}^7\text{Be}+p$  case, the  ${}^7\text{Be}\leftrightarrow{}^3\text{He}+\alpha$   $p$ -wave overlap functions have a node.

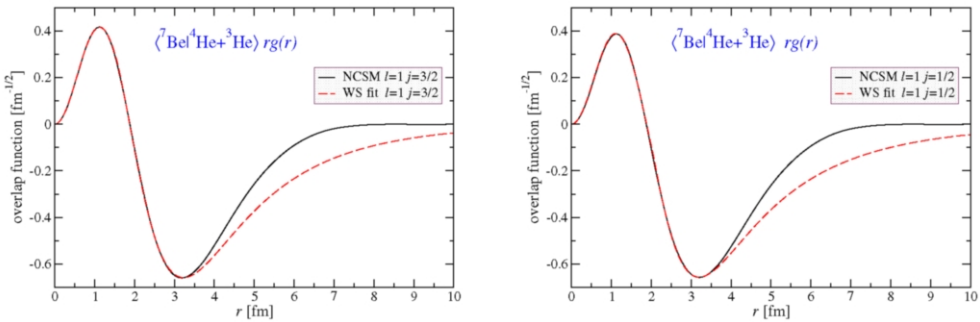


Figure 3. Left, the overlap function,  $rg(r)$ , for the first excited state of  ${}^7\text{Be}$  with the ground state of  ${}^3\text{He}$  plus  $\alpha$  as a dependence on separation between the  ${}^3\text{He}$  and the  $\alpha$  particle. The  $p$ -wave channel overlap function with  $j = 3/2$  is shown. The full line represents the NCSM result obtained using the CD-Bonn 2000 NN potential and the  $10\hbar\Omega$  model space for  ${}^7\text{Be}$  ( $12\hbar\Omega$  for  ${}^3,{}^4\text{He}$ ) with the HO frequency of  $\hbar\Omega = 13$  MeV. The dashed line represents a corrected overlap obtained with a Woods-Saxon potential whose parameters were fit to the NCSM overlap up to 3.4 fm under the constraint to reproduce the experimental separation energy. Right, the same for the  $p$ -wave channel overlap function with  $j = 1/2$ .

Using the corrected overlap functions and a  ${}^3\text{He}+\alpha$  scattering state obtained using the potential model of Ref. [22] we calculated the  ${}^3\text{He}(\alpha,\gamma){}^7\text{Be}$  S-factor. Our  $10\hbar\Omega$  result is presented in the left panel of Fig. 4. We show the total S-factor as well as the contributions from the capture to the ground state and the first excited state of  ${}^7\text{Be}$ . By investigating the model space dependence for  $8\hbar\Omega$  and  $10\hbar\Omega$  spaces (shown in the right panel of Fig. 4), we estimate the  ${}^3\text{He}(\alpha,\gamma){}^7\text{Be}$  S-factor at zero energy to be higher than 0.44 keV b, the

value that we obtained in the discussed case shown in Fig. 4. Our results are similar to those obtained by K. Nollett [23] using the variational Monte Carlo wave functions for the bound states and potential model wave functions for the scattering state.

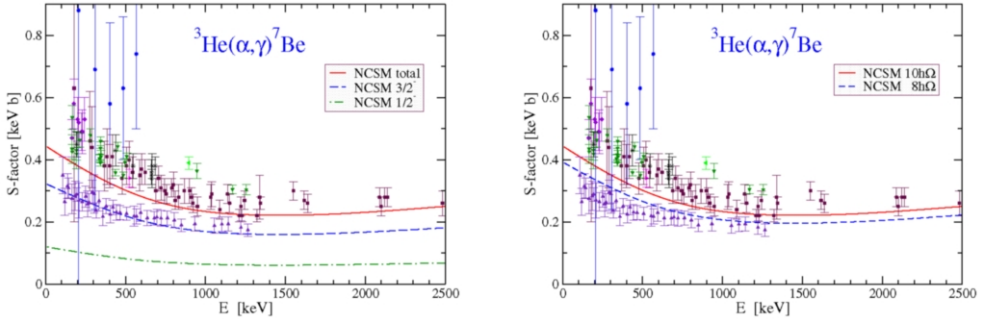


Figure 4. Left, the full line shows the  ${}^3\text{He}(\alpha,\gamma){}^7\text{Be}$  S-factor obtained using the NCSM overlap functions with corrected asymptotics. The dashed lines show the  ${}^7\text{Be}$  ground- and the first excited state contributions. The calculation was done using the CD-Bonn 2000 NN potential and the  $10\hbar\Omega$  model space for  ${}^7\text{Be}$  ( $12\hbar\Omega$  for  ${}^3,{}^4\text{He}$ ) with the HO frequency of  $\hbar\Omega = 13$  MeV. Right, the  ${}^3\text{He}(\alpha,\gamma){}^7\text{Be}$  S-factor dependence on the basis size for  ${}^7\text{Be}$   $8\hbar\Omega$  and  $10\hbar\Omega$  model spaces.

## 5. ${}^3\text{H}(\alpha,\gamma){}^7\text{Li}$ S-FACTOR

An important check on the consistency of the  ${}^3\text{He}(\alpha,\gamma){}^7\text{Be}$  S-factor calculation is the investigation of the mirror reaction  ${}^3\text{H}(\alpha,\gamma){}^7\text{Li}$ , for which more accurate data exist [24]. Our results obtained using the CD-Bonn 2000 NN potential are shown in Fig. 5. It is apparent that our  ${}^3\text{H}(\alpha,\gamma){}^7\text{Li}$  results are consistent with our  ${}^3\text{He}(\alpha,\gamma){}^7\text{Be}$  calculation. We are on the lower side of the data and we find an increase of the S-factor as we increase the size of our basis. A positive fact is that this S-factor change is rather small, a sign of convergence of our calculation.

## REFERENCES

1. E. Adelberger *et al.*, Rev. Mod. Phys. 70 (1998) 1265.
2. SNO Collaboration, S. N. Ahmed *et al.*, Phys. Rev. Lett. 92 (2004) 181301.
3. S. Couvidat, S. Turck-Chièze, and A. G. Kosovichev, Astrophys. J. 599 (2003) 1434.
4. J. N. Bahcall and M. H. Pinsonneault, Phys. Rev. Lett. 92 (2004) 121301.
5. B. W. Filippone, A. J. Elwyn, C. N. Davids, and D. D. Koetke, Phys. Rev. Lett. 50 (1983) 412; Phys. Rev. C 28 (1983) 2222.
6. L.T. Baby *et al.*, Phys. Rev. Lett. 90 (2003) 022501.
7. A. R. Junghans, E. C. Mohrmann, K. A. Snover, T. D. Steiger, E. G. Adelberger,

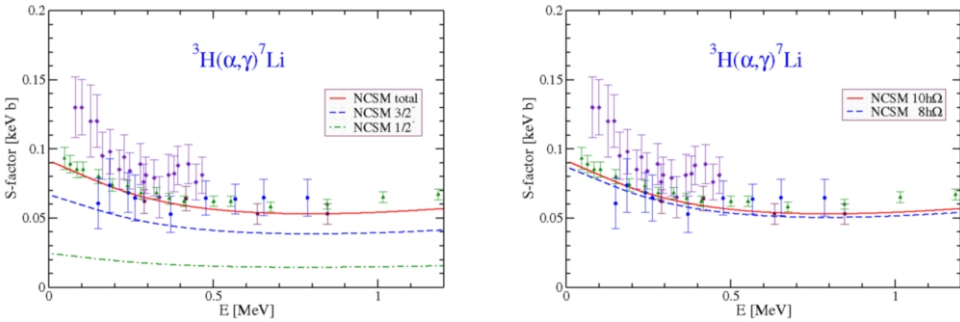


Figure 5. Left, the full line shows the  ${}^3\text{H}(\alpha,\gamma){}^7\text{Li}$  S-factor obtained using the NCSM overlap functions with corrected asymptotics. The dashed lines show the  ${}^7\text{Li}$  ground- and the first excited state contributions. The calculation was done using the CD-Bonn 2000 NN potential and the  $10\hbar\Omega$  model space for  ${}^7\text{Li}$  ( $12\hbar\Omega$  for  ${}^3\text{H}$  and  ${}^4\text{He}$ ) with the HO frequency of  $\hbar\Omega = 13$  MeV. Right, the  ${}^3\text{H}(\alpha,\gamma){}^7\text{Li}$  S-factor dependence on the basis size for  ${}^7\text{Li}$   $8\hbar\Omega$  and  $10\hbar\Omega$  model spaces.

J. M. Casandjian, H. E. Swanson, L. Buchmann, S. H. Park, A. Zyuzin, and A. M. Laird, Phys. Rev. C 68 (2003) 065803.

8. N. Iwasa *et al.*, Phys. Rev. Lett. 83 (1999) 2910; B. Davids *et al.*, Phys. Rev. Lett. 86 (2001) 2750; F. Schumann *et al.*, Phys. Rev. Lett. 90 (2003) 232501.
9. F. C. Barker, Nucl. Phys. A588 (1995) 693.
10. R. G. H. Robertson, Phys. Rev. C 7 (1973) 543.
11. S. Typel, H. H. Wolter, and G. Baur, Nucl. Phys. A613 (1997) 147.
12. B. Davids and S. Typel, Phys. Rev. C 68 (2003) 045802.
13. P. Descouvemont and D. Baye, Nucl. Phys. A567 (1994) 341.
14. A. Csoto, K. Langanke, S. E. Koonin, and T. D. Shoppa, Phys. Rev. C 52 (1995) 1130.
15. P. Descouvemont, Phys. Rev. C 70 (2004) 065802.
16. P. Navratil, J. P. Vary and B. R. Barrett, Phys. Rev. Lett. 84 (2000) 5728; Phys. Rev. C 62 (2000) 054311.
17. P. Navratil, C. A. Bertulani and E. Caurier, Phys. Lett. B 634 (2006) 191.
18. P. Navratil, C. A. Bertulani and E. Caurier, Phys. Rev. C 73 (2006) 065801.
19. R. Machleidt, Phys. Rev. C 63 (2001) 024001.
20. P. Navratil, Phys. Rev. C 70 (2004) 054324.
21. H. Esbensen and G. F. Bertsch, Nucl. Phys. A600 (1996) 37.
22. B. T. Kim, T. Izumuto and K. Nagatani, Phys. Rev. C 23 (1981) 33.
23. K. M. Nollett, Phys. Rev. C 63 (2001) 054002.
24. C. R. Brune, R. W. Kavanagh and C. Rolfs, Phys. Rev. C 50 (1994) 2205.